LBNL-41075
UC-413
Preprint

ERNEST ORLANDO LAWRENCE
BERKELEY NATIONAL LABORATORY

Z-Dependent Barriers in Multifragmentation from Poissonian Reducibility and Thermal Scaling

L. Beaulieu, L. Phair, L.G. Moretto,
and G.J. Wozniak

Nuclear Science Division

November 1997

Submitted to
Physical Review Letters

DISCLAIMER

LBNL-41075
UC-413

Z-dependent Barriers in Multifragmentation from Poissonian Reducibility and Thermal Scaling

L. Beaulieu, L. Phair, L.G. Moretto, and G. J. Wozniak

Nuclear Science Division
Ernest Orlando Lawrence Berkeley National Laboratory
University of California, Berkeley, California 94720 USA

November 1997

This work was supported in part by the Director, Office of Energy Research, Office of High Energy and Nuclear Physics, Division of High Energy Physics, of the U.S. Department of Energy under Contract No. DE-AC03-76SF00098.

Z-dependent Barriers in Multifragmentation from Poissonian Reducibility and Thermal Scaling

L. Beaulieu, L. Phair, L.G. Moretto, G.J. Wozniak

Nuclear Science Division, Lawrence Berkeley National Laboratory, Berkeley, California 94720

(November 11, 1997)

Abstract

We explore the natural limit of binomial reducibility in nuclear multifragmentation by constructing excitation functions for intermediate mass fragments (IMF) of a given element Z. The resulting multiplicity distributions for each window of transverse energy are Poissonian. Thermal scaling is observed in the linear Arrhenius plots made from the average multiplicity of each element. Emission barriers are extracted from the slope of the Arrhenius plots and their possible origin are discussed.

Typeset using REVTEX

Several aspects of nuclear multifragmentation may be understood in terms of *nearly independent* fragment emission from multifragmenting sources with *thermal-like* probabilities. It was found [1–3] that the Z integrated fragment multiplicity distributions P_n^m are binomially distributed in each transverse energy (E_t) window according to the binomial equation

$$P_n^m = \frac{m!}{n!(m-n)!}p^n(1-p)^{m-n}. \tag{1}$$

The transverse energy E_t is calculated from the kinetic energies E_i of all the charged particles in an event and their polar angles θ_i as, $E_t = \sum_i E_i \sin^2\theta_i$. The reduced one fragment emission probabilities p give linear Arrhenius plots when $\log 1/p$ is plotted vs $1/\sqrt{E_t}$. If the excitation energy E^* is proportional to E_t and consequently, the temperature T to $\sqrt{E_t}$, the linear Arrhenius plots suggest that p has the Boltzmann form $p \propto \exp(-B/T)$ [1–3].

Similarly the charge distributions for each fragment multiplicity n scale according to the equation [4]

$$\log P(Z, E_t, n) \propto \frac{B(Z)}{\sqrt{E_t}} - cnZ \tag{2}$$

where c appears to be an entropy related constant associated with the constraint of charge conservation or the lack thereof [4,5].

Also, the particle-particle angular correlation is expressible in terms of the individual fragment statistical angular distributions with their standard dependencies on the relevant moments of inertia and the temperature [6] (here, as above, taken to be proportional to $\sqrt{E_t}$).

The appeal of this comprehensive picture is marred by a number of open problems. One problem, which will be dealt with here, is that, so far, the binomial decomposition has been performed on the Z-integrated fragment multiplicities, typically associated with $3 \le Z \le 20$. Thus, the Arrhenius plot generated with the resulting one fragment probability p is an average over a range of Z values. Fortunately, it has been shown that the Arrhenius plots should survive such a Z averaging, and yield an effective barrier (slope) dominated by the lowest Z value [2,3]. However, this procedure clearly implies a substantial loss of information, and renders the binomial parameters p and m difficult to interpret.

In light of the above considerations, an analysis of the multiplicities for each fragment Z value could go a long way toward solving many of these difficulties.

Furthermore, it has been pointed out that a binomial distribution could be distorted by the averaging associated with the transformation $E \rightarrow E_t$ leading to possibly incorrect values of m and p [7]. However, it can also been shown that while p and m separately can conceivably be distorted by the transformation, the average multiplicity $\langle n \rangle = mp$ is far more resistant to the averaging process [7,8]. It would be very useful if a way could be found to avoid the individual extraction of p and m while retaining the possibility of constructing an Arrhenius plot.

In this letter, we analyze the fragment multiplicity distributions for each individual fragment Z value. We show that they are Poissonian. The associated mean multiplicities for *each* Z give linear Arrhenius plots from which the corresponding Z dependent barriers can be extracted. The physical dependence of these barriers on Z may shed light on the fundamental significance of reducibility and thermal scaling.

The effect of restricting the fragment definition to a single Z value is rather dramatic. In Fig. 1, ratios of the variance to the mean as a function of E_t are given for a number of Z values, and for the case $Z \geq 3$. For individual Z values the ratios are very close to one, while for the Z integrated case there is a pronounced sagging. The explanation for these features can be found by recalling that for a binomial distribution

$$\langle n \rangle = mp, \qquad \sigma^2 = mp(1-p), \tag{3}$$

and therefore

$$\frac{\sigma^2}{\langle n \rangle} = 1 - p. \tag{4}$$

For $p \rightarrow 0$, $\sigma^2 / \langle n \rangle = 1$. This is the Poissonian limit. When extensive summation over Z is carried out, the elementary probability p increases sufficiently at the highest values of E_t so that the distribution becomes clearly binomial. However, the restriction to any given Z value decreases the elementary probability p so dramatically that the above ratio effectively remains unity at all values of E_t and the distributions become Poissonian:

$$P_n(Z) = \frac{\langle n \rangle^n \, e^{-\langle n \rangle}}{n!}. \tag{5}$$

We can verify the quality of the Poissonian fits to the multiplicity distribution in Fig. 2. These Poissonian fits are excellent for all Z values starting from Z=3 up to Z=14 over the entire range of E_t and for all the reactions which we have studied. Thus we conclude that reducibility (we should call it now Poissonian reducibility) is verified at the level of individual Z values for many different systems. For the Xe induced reactions, there is an excellent overlap of the data sets for different targets as a function of E_t. They all follow the Poisson fit to the Au target data. The probabilities P_n and the range of E_t increase with the increasing target mass from V to Au as they must if E_t is a reasonable measure of the dissipated energy.

It should be pointed out that the experimental observation of Poissonian reducibility means that IMF production is dominated by a stochastic process. Of course stochasticity falls directly in the realm of statistical decay. It is less clear how it would fare within the framework of a dynamical model.

In order to verify thermal scaling we generate Arrhenius plots by plotting $\log \langle n \rangle$ vs $1/\sqrt{E_t}$. It is possible to use $\langle n \rangle$ directly, instead of p, since in the Poissonian limit the parameter m is lost. Fig. 3 gives a family of these plots for four different reactions. Each family contains Z values extending from Z=3 to Z=14. The observed Arrhenius plots are striking linear, and their slopes increase smoothly with increasing Z value. One notable exception is the large Z (≥ 10) data for Xe+Cu. At high E_t, the data deviates from the linear dependence observed elsewhere. It is conceivable that charge conservation constraints lead to this behaviour. But the overall linear trend demonstrates that thermal scaling is also present when individual fragments of a specific Z are considered.

The advantage of this procedure is readily apparent. For any given reaction, both Poissonian reducibility and thermal scaling are verifiable not just once, as in the previous analysis, but for as many atomic numbers as are experimentally accessible. Take for example the Ar+Au reaction (E/A=110MeV) shown in the top right panel of Fig. 3. For this specific reaction, we can verify both reducibility and thermal scaling for 12 individual atomic numbers. Since there are 29 E_t bins, Poissonian reducibility is tested 29 times for each Z value, i.e., $12 \times 29 = 348$ times for this reaction alone. Including all the cases shown in Fig. 3, we have tested Poissonian reducibility 936 times. This is an extraordinary level of verification of the empirical reducibility and thermal scaling with the variable E_t.

Two added bonuses arise from this procedure.

1) The criticism has been raised that the linearity of the Arrhenius plots arises from autocorrelation, since the complex fragments also contribute to E_t [9]. In the present analysis this criticism can be dismissed, since each individual Z contributes a vanishingly small amount to E_t.

2) The extracted elementary probability is now $\langle n \rangle = mp$ which, contrary to p and m, is very resilient to any averaging associated with the transformation from E to E_t [7,8].

It may be worth reminding the reader that this procedure does not contradict binomial reducibility. To the contrary, it represents its natural limit for small values of p, and it expands its applicability by considering each Z value individually. In going from binomial to Poissonian distributions, the price one pays is the loss of the parameter m. While in many ways this is a convenient result, it actually implies a loss of scale. In the time sequential interpretation of multifragmentation [3] this implies the loss of information about the time window during which multifragmentation occurs in units of the natural channel period, or the unit time to which the elementary probability is referred. In the space sequential interpretation, we lose information about the total mass of the source [3].

Poissonian reducibility and thermal scaling do not contradict recent observations regarding the importance of reaction dynamics in the formation of the hot primary sources [10–15]. In particular, the experimental scaling is not affected by the presence of multiple sources [3] and the analysis presented here is a powerful test to establish the degree of thermalization in the late stage of the reaction. Kinematic variables seem to retain spatial-temporal information about the reaction dynamics [11–16] while the associated emission probabilities seem to demonstrate, as verified nearly a 1000 times in the present work, the role of phase space in describing the thermalization phase of the sources.

Returning to the Arrhenius plots for individual atomic numbers, it is straightforward to obtain the values of the slopes from Fig. 3 as a function of Z. The interpretation of these slopes as emission barriers is very tempting. If we had the correct excitation energy scale, rather than E_t, we could obtain from the slopes the actual barriers as a function of Z. However, we are limited, unfortunately, to our running variable E_t and to the assumption of its proportionality to E^*. However, the many linear Arrhenius plots shown here could not be easily explained without invoking this proportionality. Still, a plot of the barriers as a function of Z is potentially rich in information. The extracted barriers are shown in Fig. 4 (bottom panel). The barriers appear to increase linearly with Z at low Z and tend to sag below linearity at higher Z values. This dependence is somewhat similar to that of the conditional barriers measured at low energy [17] (top panel). In the latter, the barrier increases only by 50% from Z=5 to the maximum at Z≈20. This range of barriers can be described by a finite range model or liquid drop parametrization [17]. In the multifragmentation data, the barriers increase by more than a factor of 2. While the Coulomb-like Z dependence of these barriers is suggestive, we should remark that these are emission barriers rather than Coulomb barriers, thus the dominance of the Coulomb term is by no means obvious.

One could speculate also on the role of surface area with respect to the origin of these barriers. Fragments might be thought as forming by coalescence into a relatively cold and dense nuclear drop out of a hot diluted source. The appearance of a substantial surface energy for the fragment would suggest barriers proportional to $Z^{2/3}$ ($A^{2/3}$). If this were true, then one would expect the barrier at each Z to be independent of the system studied. In fact, because the relation between E_t and excitation energy is unknown, the absolute values of our barriers are also unknown. By normalizing all systems at Z=6 and using the Xe+Au at E/A=50 MeV as the reference, one observes barriers that are indeed fairly independent of the system. Finally, the scaling of the barriers in Fig. 4 implies that E_t can also be rescaled for all the systems.

In conclusion, Poissonian reducibility and thermal scaling of individual fragment of a given Z have been observed experimentally for several different systems at bombarding energies ranging from 50 to 110 MeV/nucleon. The high level of verification strongly supports the stochastic/statistical nature of fragment production and provides a clear signal for source(s) thermalization in the late stage of the reaction. "Emission" barriers were extracted from the Arrhenius plots. The rate of change of these barriers with Z compared to those measured at low energy, and the scaling for the different systems suggest a surface origin. If the physical significance of these Z dependent barriers must remain lamentably open, there is at least the hope that important physical information is contained therein. Data with isotopically resolved light charged particles and IMFs are needed to futher investigate these phenomena.

Acknowledgements

This work was supported by the Director, Office of Energy Research, Office of High Energy and Nuclear Physics, Nuclear Physics Division of the US Department of Energy, under contract DE-AC03-76SF00098. One of us (L.B) acknowledge a fellowship from the National Sciences and Engineering Research Council (NSERC), Canada.

REFERENCES

[1] L.G. Moretto *et al.*, Phys. Rev. Lett. **74**, 1530 (1995).

[2] K. Tso et al., Phys. Lett. B **361**, 25 (1995).

[3] L.G. Moretto, *et al.*, Phys. Rep. **287**, 249 (1997).

[4] L. Phair et al., Phys. Rev. Lett. **75**, 213 (1995).

[5] L.G. Moretto et al., Phys. Rev. Lett. **76**, 372 (1996).

[6] L. Phair *et al.*, Phys. Rev. Lett **77**, 822 (1996).

[7] J. Toke *et al.*, Phys. Rev. C **56**, R1683 (1997).

[8] L. Phair *et al.*, to be published.

[9] M.B. Tsang *et al.*, MSU preprint MSU-1069.

[10] C.P. Montoya *et al.*, Phys. Rev. Lett **73**, 3070 (1994).

[11] Y. Larochelle *et al.*, Phys. Rev. C **55**, 1869 (1997).

[12] J. Lukasik *et al.*, Phys. Rev. C **55**, 1906 (1997).

[13] J. Toke *et al.*, Phys. Rev. Lett. **75**, 2920 (1995).

[14] J.F. Lecolley *et al.*, Phys. Lett. B **354**, 202 (1995).

[15] J.F. Dempsey *et al.*, Phys. Rev. C **54**, 1710 (1996).

[16] D.R. Bowman *et al.*, Phys. Rev. Lett **70**, 3534 (1993).

[17] K.X. Jing *et al.*, LBNL-40779, submitted to Phys. Rev. C.

FIGURES

FIG. 1. The ratio of the variance to the mean number of Li, C, O and Ne (solid and open symbols) emitted from the reaction ^{36}Ar+^{197}Au at E/A=110 MeV. The star symbols show the same ratio for all IMFs ($3 \leq Z \leq 20$).

FIG. 2. The excitation functions P_n for carbon emission (left column) and neon emission (right column) from the reactions ^{36}Ar+^{197}Au at E/A=110 MeV (top panels) and ^{129}Xe+^{51}V,^{nat}Cu,^{89}Y,^{197}Au (bottom panels). The lines are a Poisson fit to the gold target data.

FIG. 3. The average yield per event of the different indicated elements (symbols) as a function of $1/\sqrt{E_t}$ for four different reactions. The lines are linear fits to the data.

FIG. 4. Top panel: Experimental emission barriers for ^{94}Mo from the ^{82}Kr+^{12}C reactions between 5.0 and 12.7 MeV/nucleon. of ref [17]. Bottom panel: The Z dependent "barriers" (the slope of the Arrhenius plots of Fig. 3) . The barriers have been scaled relative to Z=6 of the Xe+Au data.

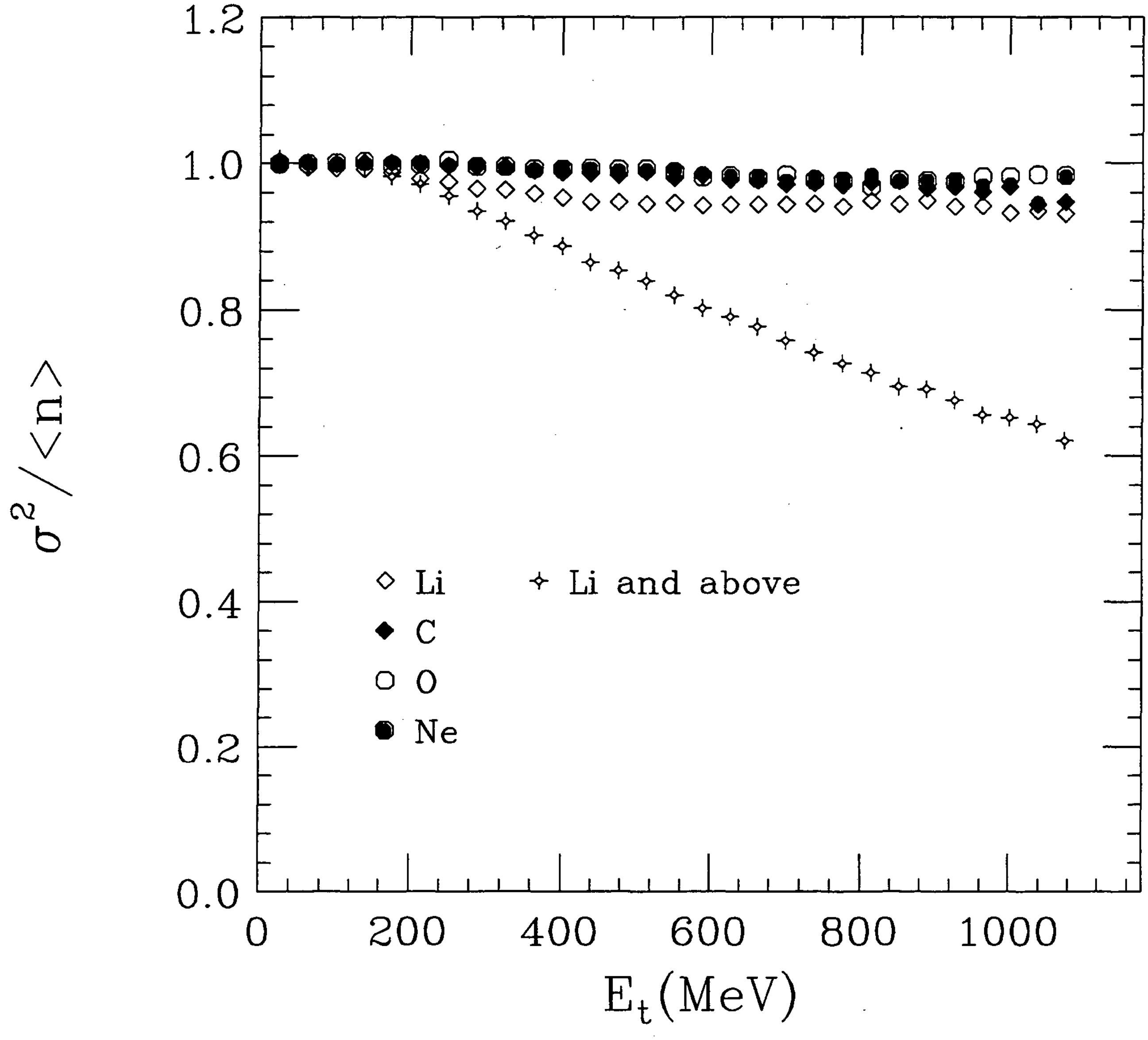

FIG. 1. L. Beaulieu *et al.*

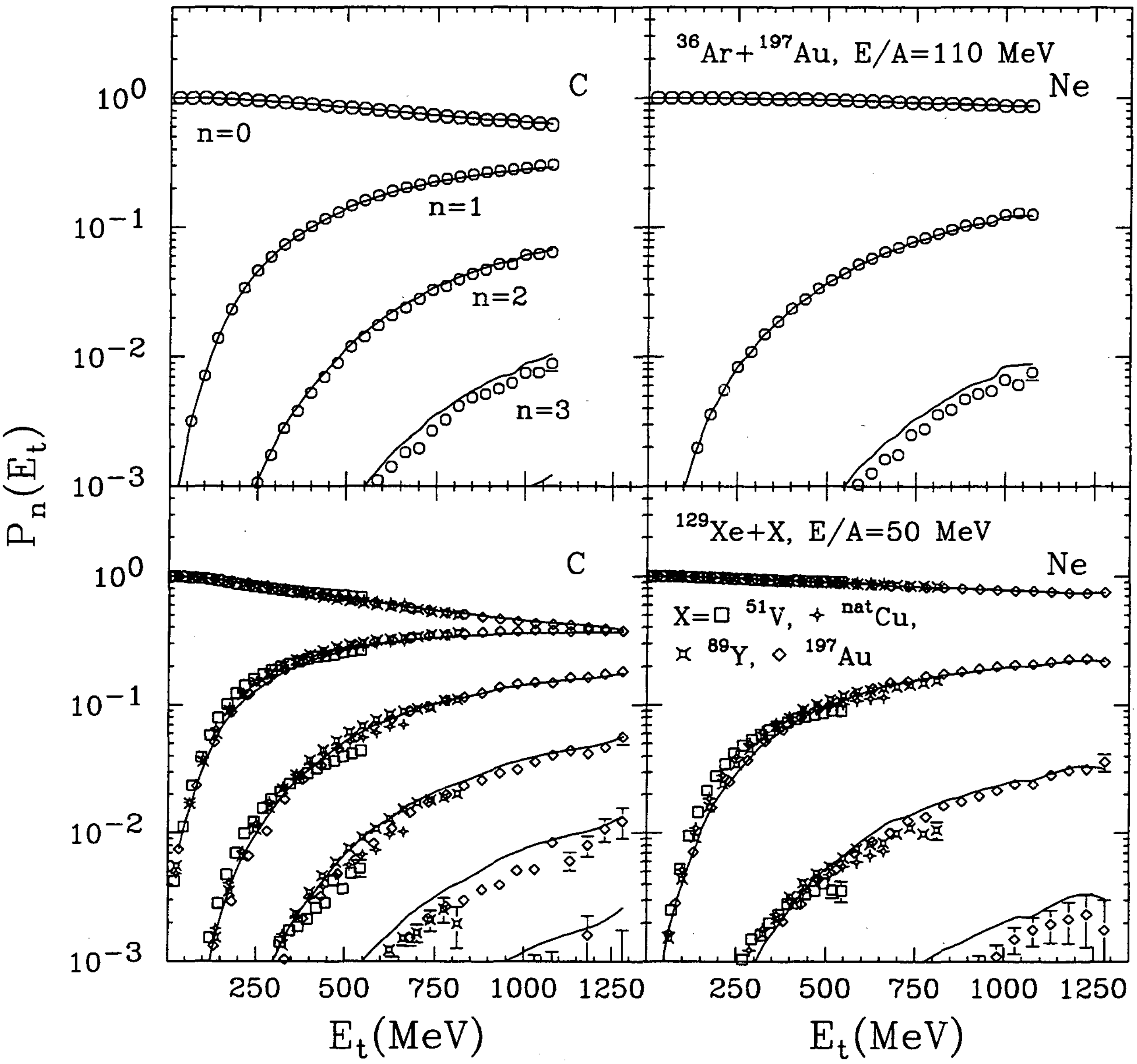

FIG. 2. L. Beaulieu *et al.*

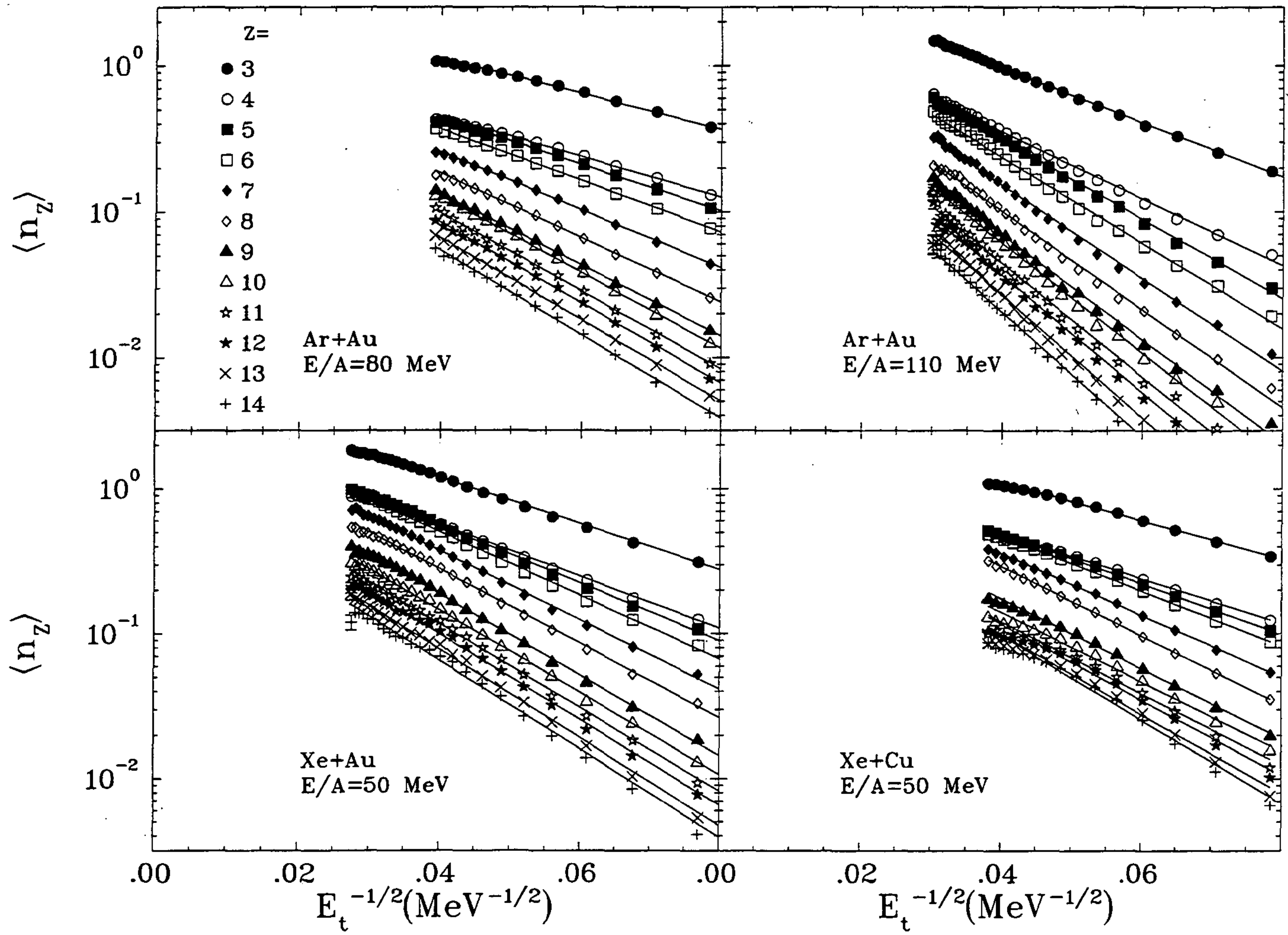

FIG. 3. L. Beaulieu *et al.*

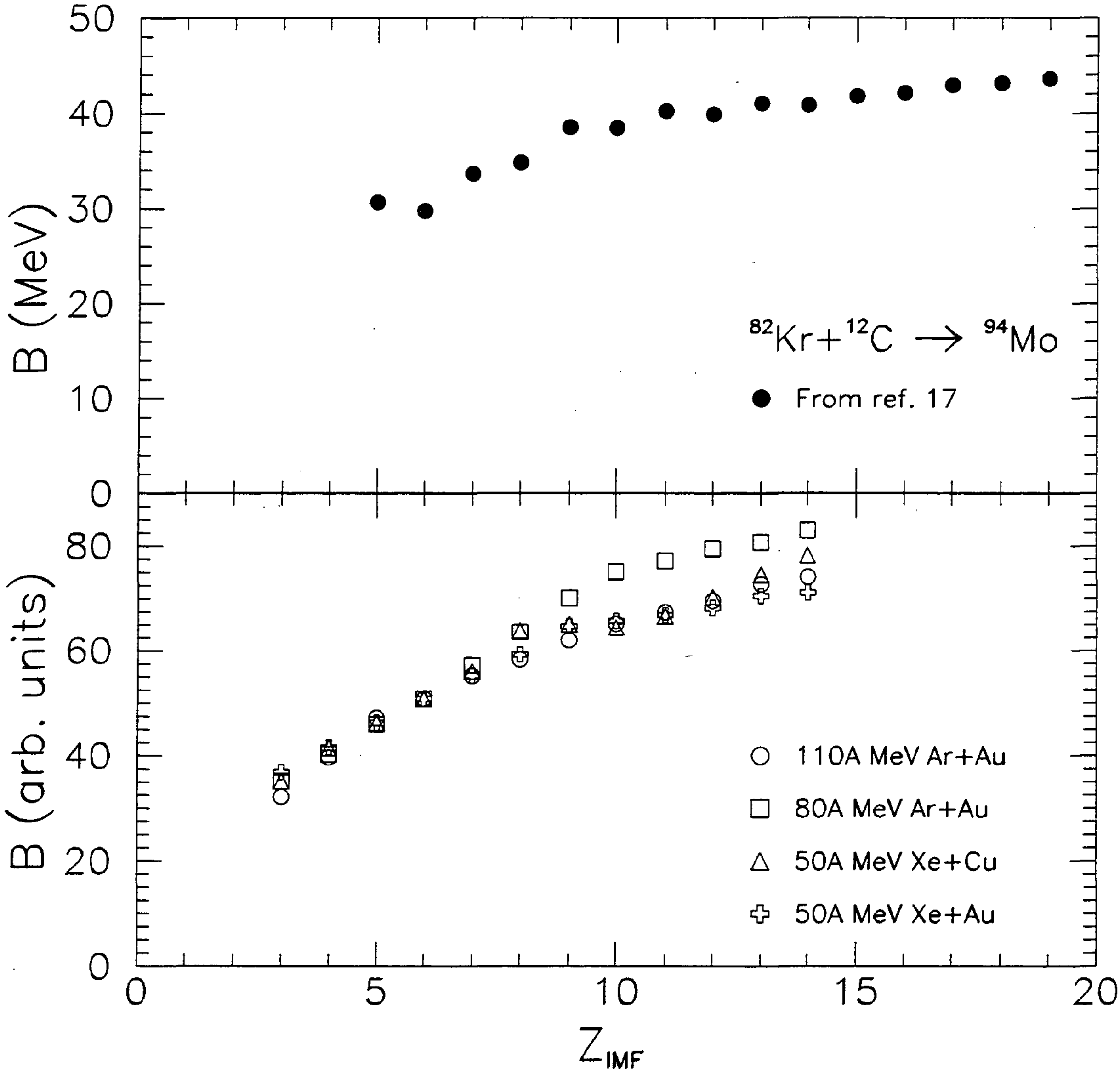

FIG. 4. L. Beaulieu *et al.*

Ernest Orlando Lawrence Berkeley National Laboratory
One Cyclotron Road | Berkeley, California 94720

Prepared for the U.S. Department of Energy under Contract No. DE-AC03-76SF00098